AD-A172 549 FRACTURE TOUGHNESS OF FIBER REINFORCED CONCRETE(U) 1/1
NORTHWESTERN UNIV EVANSTON IL DEPT OF CIVIL ENGINEERING
S P SHAH 01 NOV 85 AFOSR-TR-86-0898 AFOSR-82-0243
UNCLASSIFIED F/G 11/2 NL

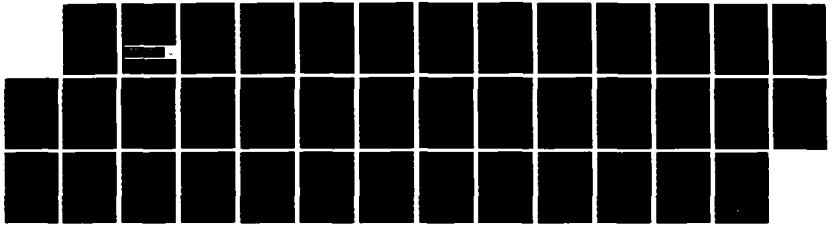

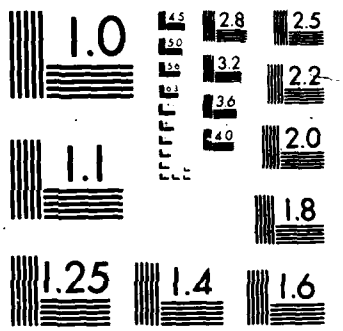
1.0
1.1
1.25
1.4
1.6
1.8
2.0
2.2
2.5
2.8
3.2
3.6
4.0
4.5
5.0
5.6
6.3

AFOSR-TR- 86-0898

898

(2)

AD-A172 549

Final Report

Fracture Toughness of
Fiber Reinforced Concrete

AFOSR - 82-0243

Principal Investigator: S. P. Shah

Technological Institute
NORTHWESTERN UNIVERSITY
EVANSTON, ILLINOIS

AFOSR-TR- 86-0898

Final Report

Fracture Toughness of Fiber Reinforced Concrete

AFOSR - 82-0243

Principal Investigator: S. P. Shah

Approved for public release;
distribution unlimited.

AIR FORCE OFFICE OF SCIENTIFIC RESEARCH (AFSC)
NOTICE OF TRANSMITTAL TO DTIC
This technical report has been reviewed and is approved for public release IAW AFR 190-12.
Distribution is unlimited.
MATTHEW J. KERPER
Chief, Technical Information Division

Unclassified

SECURITY CLASSIFICATION OF THIS PAGE

AD-A172549

REPORT DOCUMENTATION PAGE

1a. REPORT SECURITY CLASSIFICATION: Unclassified	1b. RESTRICTIVE MARKINGS
2a. SECURITY CLASSIFICATION AUTHORITY	3. DISTRIBUTION/AVAILABILITY OF REPORT: Approved for Public Release; Distribution Unlimited
2b. DECLASSIFICATION/DOWNGRADING SCHEDULE	
4. PERFORMING ORGANIZATION REPORT NUMBER(S)	5. MONITORING ORGANIZATION REPORT NUMBER(S): AFOSR-TR- 86-0898
6a. NAME OF PERFORMING ORGANIZATION: Northwestern University Civil Engineering Department; 6b. OFFICE SYMBOL (If applicable)	7a. NAME OF MONITORING ORGANIZATION: AFOSR
6c. ADDRESS (City, State and ZIP Code): Evanston, IL 60201	7b. ADDRESS (City, State and ZIP Code): Same as 8c
8a. NAME OF FUNDING/SPONSORING ORGANIZATION: Air Force Office of Scientific Research; 8b. OFFICE SYMBOL (If applicable): AFOSR/NA	9. PROCUREMENT INSTRUMENT IDENTIFICATION NUMBER: AFOSR-82-0243
8c. ADDRESS (City, State and ZIP Code): Bolling AFB, DC 20332	10. SOURCE OF FUNDING NOS.
11 TITLE (Include Security Classification)	PROGRAM ELEMENT NO.: (illegible)021; PROJECT NO.: 2307; TASK NO.: C9; WORK UNIT NO:
12. PERSONAL AUTHOR(S): Shah, Surendra P.	
13a. TYPE OF REPORT: FINAL; 13b. TIME COVERED: FROM 6/82 TO 8/85; 14. DATE OF REPORT (Yr., Mo., Day): 1985/11,1; 15. PAGE COUNT: 36	
16. SUPPLEMENTARY NOTATION	

17 COSATI CODES			18. SUBJECT TERMS (Continue on reverse if necessary and identify by block number)
FIELD	GROUP	SUB. GR	

19. ABSTRACT (Continue on reverse if necessary and identify by block number)

See 1. Summary

20 DISTRIBUTION/AVAILABILITY OF ABSTRACT: UNCLASSIFIED/UNLIMITED ☒ SAME AS RPT ☐ OTIC USERS ☐	21 ABSTRACT SECURITY CLASSIFICATION
22a. NAME OF RESPONSIBLE INDIVIDUAL: Lt. Col. Lawrence D. Hokanson	22b TELEPHONE NUMBER (Include Area Code): (202)767-4935; 22c OFFICE SYMBOL: AFOSR/NA

DD FORM 1473, 83 APR EDITION OF 1 JAN 73 IS OBSOLETE.

SECURITY CLASSIFICATION OF THIS PAGE

1. Summary

The primary accomplishment during the reporting period was the development of nonlinear fracture criteria for cement-based composites. These fracture criteria accurately predict two important aspects of crack growth in concrete, fiber reinforced concrete and other cement-based composites: nonlinear process zone and quasi-stable crack growth beyond the peak load. A preexisting crack in a concrete structure propagates in two stages: subcritical crack growth, and beyond the peak load, post-critical crack growth. The second stage can only be observed if the structure is loaded in a displacement-controlled mode. As a result of the nonlinear subcritical crack growth, when the fracture toughness of a concrete specimen (for example, notched-beam) is determined using conventional linear elastic fracture mechanics, different values are observed depending upon the size of the specimen.

A size independent critical stress intensity factor and critical crack-tip opening displacement are proposed as fracture toughness criteria for the concrete. To evaluate these two parameters, nonlinear deformations must be extracted from the total displacement. How to evaluate these two parameters from the three-point notched beam test is detailed in the attached paper.

Notched-beam specimens of three different sizes and five different materials composites were tested to develop the proposed theoretical model. Beams were tested in a closed-loop testing system using the crack mouth opening displacement as a feed-back control. Crack growth was microscopically monitored. It was observed that the nonlinear critical stress intensity factor (as defined here) was independent of the size of the specimen and was constant during the post-critical crack growth.

Based on the above proposed fracture criteria (critical stress intensity factor and critical crack tip opening displacement), the fracture behavior of

steel fiber reinforced concrete can be simulated by incorporating the bridging effect of steel fibers. The mechanism of fracture resistance can be separated into three stages as: subcritical crack growth in matrix and beginning of fiber bridging effect; post critical crack growth in matrix such that the net stress intensity factor due to the applied load and fiber bridging force remains constant; and a final stage where the resistance to crack separation is provided exclusively by fibers. A theoretical model is proposed to predict the fracture behavior of fiber reinforced concrete based on the aforementioned fracture mechanisms. The proposed model is detailed in the attached paper.

In addition to the fracture mechanics based model, a micromechanics based model was developed to predict the tensile stress-strain response of fiber reinforced composites. This model incorporates the inelastic behavior of the fiber-matrix interface and the softening characteristics of the matrix. The model is sensitive to parameters such as volume fraction and aspect ratio and modulus of elasticity of fibers.

For fiber reinforced cement based composites, the bond between fiber and matrix is relatively weak and hence it critically influences the performance of the composite. The bond properties are generally determined from a single fiber pullout test. To determine bond strength from the observed maximum pullout load, it is usually assumed that the interfacial shear stresses are uniformly distributed along the embedded length of the fiber. An alternate interpretation of the pullout test based on fracture mechanics concept was developed in this study. In this model, the interface is characterized by its specific work of pullout fracture rather than shear strength.

2. Research Objective

To develop rational methods to predict fracture toughness of fiber reinforced concrete is the primary goal of this investigation. It is known that the addition of randomly distributed, short, steel fibers substantially enhances the crack propagation resistance of concrete. How to experimentally evaluate this critical property of fiber reinforced concrete and how to rationally predict it are the objectives of this research.

3. List of Publications

1. Wecharatana, M., and S. P. Shah, "A Model for Predicting Fracture Resistance of Fiber Reinforced Concrete," Cement and Concrete Research, November 1983, pp. 819-830.

2. Ballarini, R., S. P. Shah, and L. M. Keer, "Crack Growth in Cement Based Composites," Engineering Fracture Mechanics, Vol. 20, No. 3, 1984, pp. 433-485.

3. Jenq, Y. S., and S. P. Shah, "A Fracture Toughness Criterion for Concrete," Engineering Fracture Mechanics, Vol. 21, No. 5, 1985, pp. 1055-1069.

4. Jenq, Y. S., and S. P. Shah, "Nonlinear Fracture Mechanics for Cement Based Composites: Theory and Experiments," Proceedings of the NATO-ARW on Applications of Fracture Mechanics to Cementitious Composites, Sept. 4-7, 1984, Northwestern Univeristy, Ed., S. P. Shah, Martinus Nijhoff, 1985.

5. Ballarini, R., S. P. Shah, and L. M. Keer, "Nonlinear Analysis for Mixed Mode Fracture," Proceedings of the NATO-ARW on Applications of Fracture Mechanics to Cementitious Composites, Sept. 4-7, 1984, Northwestern University, Ed., S. P. Shah, Martinus Nijhoff, 1985.

6. Stang, H., and S. P. Shah, "Failure of Fiber Reinforced Composites by Pull-Out Fracture," Journal of Materials Science, to be published.

7. Jenq, Y. S., and S. P. Shah, "Crack Propagation in Fiber Reinforced Concrete," Journal of Structural Engineering, (ASCE), to be published.

8. Jenq, Y. S., and S. P. Shah, "A Measure for the Fracture Toughness of Cement Based Materials," Proceedings, Symposium L. The Potential for Very High Strength Cement Based Materials., Materials Research Society, Boston, Nov. 26-30, 1984.

9. Ballarini, R., "An Analytical and Experimental Investigation of a Two Dimensional Anchor Pull-Out Test," Ph.D. dissertation, Northwestern University, 1985.

10. Jenq, Y. S., and Shah, S. P., "Fracture Toughness of Fiber Reinforced Concrete," Proceedings of the Second Symposium on the Interaction of Non-Nuclear Munitions with Structures, University of Floriada, April 1985.

11. Shah, S. P., and Jenq, Y. S., "Fracture Resistance of Steel Fiber Reinforced Concrete," U.S.-Sweden Seminar on Steel Fiber Reinforced Concrete, Stockholm, Sweden, June 1985.

12. Shah, S. P., "Dependence of Concrete Fracture Toughness on Specimen Geometry and on Composition," Fracture Mechancis of Concrete, Carpinteri, A. and Ingraffea, A. R. (editors), Martinus Nijhoff Publishers, 1984, pp. 111-133.

13. Shah, S. P., "Fracture of Cement and Concrete," Proceedings of Sixth International Conference on Fracture, New Delhi, India, 1984, pp. 495-505.

14. Shah, S. P., "Experimental and Analytical Methods to Determine Fracture Parameters for Concrete," Transactions of the 7th International Conference on Structural Mechanics in Reactor Technology, Chicago, August 1983.

15. Jenq, Y. S. and Shah, S. P., "Application of Two Parameter Fracture Model to Concrete and Fiber Reinforced Concrete," Proceedings of the International Conference on Fracture Mechanics of Concrete, Lausanne, Switzerland, October 1985.

16. Stang, H. and Shah, S. P., "Fracture Mechanical Interpretation of the Fiber/Matrix Debonding Process in Cementitious Composites," Proceedings of the International Conference on Fracture Mechanics of Concrete, Laussane, Switzerland, October 1985.

17. Ballarini, R. Shah, S. P., and Keer, L. M., "Failure Characteristics of Short Anchor Bolts Embedded in a Brittle Material," to be published in the Proceedings of the Royal Society, Paper No. 85A65.

18. Gopalaratanam, V., and Shah, S. P., "Tensile Fracture of Steel Fiber Reinforced Concrete," Division of Structural Engineering, ASCE, Submitted for publication.

4. List of Professional Collaborators

Y. S. Jenq	Ph.D. Candidate
R. Ballarini	Ph.D. (1985)
A. Anandarajah	Post-doctoral Research Fellow
V. S. Gopalaratanam	Ph.D. (1985)
H. Stang	Post-doctoral Research Fellow
M. Wecharatana	Ph.D. (1982)
L. M. Keer	Professor

5. Technical Presentations at the Following Professional Meetings

1. IUTAM William Prager Symposium on "Mechanics of Geomaterials: Rocks, Concretes, Soils," Northwestern University, September 1983.

2. Annual Convention of American Society of Civil Engineers - Structure Congress, Houston, October 17-19, 1983.

3. Annual Meeting, Transportation Research Board, Washington, D. C., January 1984.

4. NATO-Advanced Research Workshop on "Application of Fracture Mechanics to Cementitious Composites," Northwestern University, September 1984.

5. Symposium on the Potential for Very High Strength Cement Based Materials, Annual Meeting of Materials Research Society, Boston, November 1984.

6. Second Symposium on the Interaction of Non-Nuclear Munitions with Structures, Panama City, Florida, April 15-19, 1985.

7. International Conference on Fracture Mechanics of Concrete, Laussane, Switzerland, October 1985.

8. U.S.A. - Sweden Seminar on Steel Fiber Reinforced Concrete, Stockholm, Sweden, June 1985.

9. Sixth International Conference on Fracture, New Delhi, India, 1984.

10. 7th International Conference on Structural Mechanics in Reactor Technology, Chicago, 1983.

7. Additional Information

A paper which summarizes our fracture mechanics model for steel fiber reinforced concrete as well as for plain concrete is attached. This paper is accepted for publication in Journal of Structural Division (ASCE).

CRACK PROPAGATION OF FIBER REINFORCED CONCRETE

By

Y. S. Jenq and S. P. Shah
(accepted for publication in Journal of Structural Engineering)

ABSTRACT

A fracture mechanics based theoretical model is presented to predict the crack propagation resistance of fiber reinforced cement based composites. Mode I crack propagation and steel fibers are treated in the proposed model. The mechanism of fracture resistance for FRC can be separated as: subcritical crack growth in matrix and beginning of fiber bridging effect; post critical crack growth in matrix such that the net stress intensity factor due to the applied load and the fiber bridging closing stresses remain constant; and a final stage where the resistance to crack separation is provided exclusively by fibers. The response of FRC during all these stages was successfully predicted from the knowledge of matrix fracture properties and the pull-out load vs. slip relationship of single fiber. The model was verified with the results of experiments conducted on notched beams reported here as well as by other researchers. Beams were loaded in a closed-loop testing machine so as to maintain a constant rate of crack mouth opening displacement.

Introduction

Research conducted during the last twenty years has shown that the addition of fibers significantly improves penetration, scabbing and fragmentation resistance of concrete. The possible applications of fiber reinforced concrete (FRC) include explosion and shock resistant protective structures. Even though the enhanced "cracking resistance" is the most important attribute of FRC, there are no rational methods of measuring or predicting this important material property.

For fiber reinforced cement based composites, the principal beneficial

effects of fibers accrue after the cracking of matrix has occurred. For loads beyond which the matrix has initially cracked, the further crack extension and opening is resisted by bridging of fibers across the crack. Many investigators have used fracture mechanics concepts, [1,3,5,6,11,13,18,19] to incorporate the effects of fibers bridging.

In this paper a fracture mechanics based theoretical model is presented. To aid in development of the proposed theoretical model, experiments were conducted on unreinforced and steel fiber reinforced notched-beam specimens of various sizes. Beams were loaded in a closed-loop testing machine so as to maintain a constant rate of crack mouth opening displacement (CMOD).

PROPOSED MODEL FOR CRACK PROPAGATION

The proposed model can be described by considering the load vs crack mouth opening displacement relationship of a notched beam shown in Fig. 1. The critical load carrying capacity of the unreinforced matrix is assumed to reach when the stress intensity factor K_{Ic}^{S} is attained. This K_{Ic}^{S} is not the conventional stress intensity factor because of the nonlinear crack growth that preceeds the critical load (Fig. 1). To calculate the critical stress intensity factor, the inelastic displacement are separated from the total response and it is assumed that the effective slow crack growth (also often termed process zone) (ℓ_{ec}) is related to the critical value of the crack tip opening displacement ($CTOD_c$). The method of calculating K_{Ic}^{S} and $CTOD_c$ is described later.

Beyond the critical load if the unreinforced structure is loaded at a moderate rate in the displacement control model, then the crack propagates in a "steady state" manner such that the stress intensity factor continues to be equal to K_{Ic}^{S} as depicted in Fig. 1.

For fiber reinforced composites, the crack propagation in the matrix is assumed to be governed by the same criteria as those for unreinforced ma-

trix. However, the fiber-bridging effect must be included in calculating the imposed stress intensity factor (K_I). The total load P acting on the composite can be divided into three parts (Fig. 2):

$$P = P^M + P_k^f + P_s^f \tag{1}$$

where P^M is the contribution due to matrix and is related to K_I, P_k^f is related to K_I^f and accounts for the singularity effect due to fiber bridging, and P_s^f satisfies global equilibrium due to fiber bridging forces (Fig. 2).

Note that the value of P for FRC does not necessarily attain a maximum when K_I just reaches K_{Ic}^s. Depending upon the volume of fibers, the maximum load for FRC may occur for a larger crack length than that corresponding to the peak load of the unreinforced matrix (Fig. 1). Beyond this load, the cracks in FRC continue to extend while maintaining $K_I = K_{Ic}^s$, the corresponding value of P can be determined using the proposed model (Eq. 1).

When the crack mouth opening displacement (CMOD in Fig. 1) becomes very large, the resistance offered by matrix becomes negligible and eventually the stress intensity factor (K_I) becomes zero. Further crack separation is now mainly resisted by fibers. At this stage the load (P) and the corresponding CMOD can be calculated from only the global equilibrium consideration. That is:

$$P = P_s^f \tag{2}$$

The beginning of this stage is assumed to be reached when the CMOD of FRC reaches CMOD for unreinforced matrix at the point where the load in the post-peak region is 5% of the maximum load (Fig. 1). At this CMOD it was assumed that K_I suddenly becomes zero instead of its prior value of K_{Ic}^s. In reality the stress concentration value gradually diminishes: this transition zone was not considered in the proposed model.

EXPERIMENTAL DETERMINATION OF CRITICAL STRESS INTENSITY FACTOR (K_{Ic}^s) AND CRITICAL CRACK TIP OPENING DISPLACEMENT ($CTOD_c$)

The proposed model is applicable in general to specimens or structures of any geometry. To experimentally verify and numerically demonstrate the model, notched beam specimens which were simply supported and centrally loaded (the so-called three-point bend specimen) were tested. To demonstrate the validity of K_{Ic}^s and $CTOD_c$ as valid material parameters, unreinforced specimens of varying sizes and made with cement paste, mortar and concrete were tested [7,8]. Here, only the results of one series of mortar specimens which had somewhat similar composition as the fiber reinforced mortar specimens to be described later are reported.

Dimensions of specimens are reported in Table 1. For each specimen size, some specimens were loaded monotonically while some were loaded and unloaded repeatedly. The load was applied so as to maintain a constant rate of increase of CMOD.

As a result of the nonlinear slow crack growth prior to the peak load one cannot use the initial notch length (a_0) to calculate the critical stress intensity factor from the measured maximum load and using LEFM. An effective crack length ($a = a_0 + \ell_{ec}$) was defined such that the measured elastic crack mouth opening displacement ($CMOD^e$) and that calculated using this length, measured load and using LEFM were equal. Once the effective crack length is determined (an iterative procedure was employed) then the values of K_{Ic}^s and critical crack tip opening displacement [Fig. 3a] ($CTOD_c$) can be calculated using LEFM. The linear elastic fracture mechanics (LEFM) based formuli used to relate the measured load (P_{max}), $CMOD^e$, $CTOD_c$, and K_{Ic}^s for the notched beam geometry used here are given in the Appendix [9, 16].

The values of K_{Ic}^s and $CTOD_c$ for three different geometries of mortar are shown in Table 1 along with some other relevant information. It can be ob-

served that the value of K_{Ic}^s calculated as proposed is essentially independent of the geometry of the beam specimens. The size independency of the proposed K_{Ic}^s was also demonstrated for beam specimens of concrete and cement paste. tested by the authors as well as by other investigators [7-9].

The values of the critical crack tip opening displacement for mortar specimens ($CTOD_c$) are shown in Table 1. The values of the critical crack tip opening displacement were not consistently the same for different sizes of beams for all mix-proportions. However, it was assumed that they can be considered independent of the dimension of the beams.

It should be noted that the critical strain energy release rate (G_{Ic}^s) is not equal to $(K_{Ic}^s)^2/E'$ because of the nonlinear energy absorbed at crack front (in the process zone) as well as energy absorbed in the noncritical region. This can be seen when comparing G_{Ic}^s value in Table 1 with the measured value of G_F which was the total measured area under the entire load-deflection curve. This additional nonlinear energy was shown to depend on the geometry of the specimen [7]. For fiber reinforced composites, since the contribution of the matrix fracture energy is small compared to that provided by fibers pulling out, it was assumed that the total fracture energy of matrix can be obtained by simply multiplying G_{Ic}^s by a constant C. The value of this constant obtained from the ratio G_F/G_{Ic}^s is shown in Table 1.

RESISTANCE PRODUCED BY FIBERS

The resistance offered by fibers (only steel fibers are considered here) depends primarily on the interfacial bond between the fibers and the matrix. This is because of the short length (of the order of 25mm) of the fibers and rather weak zone in the matrix that is observed surrounding the fibers [4]. It is assumed that the fiber-bridging forces can be calculated from the pull-out test results of single, aligned fiber. Load-slip relationship of the two types of steel fibers observed from pull-out tests are shown in Fig. 4. The

result shown for Fig. 4a refers to the fiber with the hooks at the ends while Fig. 4b is for straight fiber. It can be seen that for both types of fibers the initial debonding region is followed by fibers pulling out of the matrix. When the total observed slip was equal to the embedment length (which was half the length of the fiber) the load drops to zero. For both types of fibers, the initial debonding can be approximated by a vertical straight line up to the maximum load. With this approximation, the load-slip curve can be represented by:

$$\frac{\sigma(w)}{\sigma_{max}} = \left[1 - \frac{w}{w_{max}}\right]^{m}, \qquad 0 \leq w \leq w_{max} \tag{3}$$

where σ_{max} is the maximum load divided by the total cracked area, w = slip or crack opening displacement, w_{max} = slip at zero load which can be assumed to be half the length of the fiber, and $\sigma(w)$ is the load at any given slip divided by the cracked area and is termed fiber pull-out stress, or the fiber bridging closing pressure and m is constant which depends on the type of fibers and was assumed to be 2 for the straight fibers used in this investigation [2,10,12,15].

The maximum pull-out strength, σ_{max} will depend on the number of fibers crossing the cracked surfaces, that is, on the volume fraction of fibers. In actual composites, fibers are not aligned but have random spatial distribution; this will influence the value of σ_{max} [12]. To account for the spatial distribution of fibers an effective volume fraction of fibers (v_{ef}) was used in this study. Based on single fiber pull-out tests of straight steel fibers, the following value for σ_{max} was used:

$$\begin{aligned} \sigma_{max} &= 240\ v_{ef} \quad \text{psi} \\ &= 1.655\ v_{ef} \quad \text{MPa} \end{aligned} \tag{4}$$

The determination of v_{ef} was empirical and is described later.

CALCULATION OF LOAD-CMOD CURVES FOR FIBER REINFORCED COMPOSITES

From the knowledge of K^s_{Ic} , $CTOD_c$ and the fiber closing pressure vs. slip relationship determined from the pull-out test one can calculate the entire load vs. CMOD and load vs. deflection relationships. The detailed equations and procedures are given in the Appendix.

The procedure involves calculating the applied load and the corresponding CMOD for a given value of the effective crack extension (ℓ_e) . The procedures outlined below are repeated for different increments of ℓ_e to obtain the entire P - CMOD response.

1. Calculation of critical effective crack extension (ℓ_{ec})

From the given material parameters, K^s_{Ic} and $CTOD_c$, one can calculate the critical effective crack extension (ℓ_{ec}) for the unreinforced matrix using LEFM based formulae by solving Eqs. A1, A2 and A3 for the notched-beam geometry used. It is assumed that the value of ℓ_{ec} remains unchanged when fibers are used.

2. Calculation of net stress intensity factor (K_I) for a given value of ℓ_e

If a given value of ℓ_e is less than ℓ_{ec} then K_I is less than K^s_{Ic} ; and if $\ell_e > e_{ec}$ then $K_I = K^s_{Ic}$. For the precritical crack growth the relationship between ℓ_e and K_I was assumed as described in Eq. A4 (Appendix).

3. Calculation of $CMOD^e$ and P^M

For the given vlaue of ℓ_e and K_I, one can calculate P^M and $CMOD^e$ using Eqs. A1 and A2.

4. Calculations of CMOD from $CMOD^e$

Note that the total crack mouth opening displacement (CMOD) includes both the elastic and the inelastic components. An empirical relation was derived from the load-unload tests on unreinforced matrix. This

relationship is given in Appendix (Eqs. A5 to A7).

5. Calculation of fiber-bridging closing pressure

For a given value of CMOD, the closing pressure can be calculated using Eqs. 3 and 4 and from the knowledge of the crack profile. An assumption of a straight crack profile was found to be sufficiently accurate.

6. Calculation of K_I^f

To calculate the stress intensity factor due to the fiber bridging closing pressure (K_I^f) the procedures described in Appendix (d) were used.

7. Calculation of P_k^f

The value of the load P_k^f can be calculated from the known value of K_I^f and the LEFM based equation (Eq. A2).

8. Calculation of P_s^f

The value of P_s^f is determined using global equilibrium condition as illustrated in Fig. A3 and detailed in Appendix (e).

9. Calculation of total applied load

The total applied load corresponding to the given value of ℓ_e is the sum of P^M, P_k^f and P_s^f .

CALCULATIONS OF LOAD-DEFLECTION RESPONSE OF FRC

To relate the loads with the load-point deflection, the concept of global energy balance was used. The total strain energy release rate (termed G_R) for the critical section can be derived as:

$$G_R = \frac{d}{da}(W = W_e + W_p) \approx C\frac{K_I^2}{E'} + \int_0^{CTOD} \sigma(w)\, dw \qquad (5)$$

where W_e and W_p are the elastic and inelastic energies consumed during the formation of new crack, K_I = net stress intensity factor due to applied load and closing pressure, CTOD = crack opening displacement at the original crack

tip, (Fig. 3), and C = energy correction factor for the plain matrix as indicated earlier. From Eq. 5 one can calaulate G_R for a given ℓ_e (and thus given K_I, CMOD and CTOD (Eq. A3)) and obtain the so-called crack-resistant curve or R-curve (Fig. 5).

For a certain amount of increment of effective crack extension, the total energy absorbed determined from G_R vs. ℓ_e is equated to that obtained from the load vs. load-point deflection curve (shaded areas in Fig. 5). From this equality and knowing the R-curve, load-point deflections can be determined. It was assumed that unloading was elastic prior to peak, whereas for load-deflection curve beyond the peak, it was assumd that the elastic deflection after unloading remained constant and was equal to that at the peak (Fig. 5).

TEST PROGRAM

Three point bend test was used to verify the validity of the proposed model. Fiber reinforced beams with dimensions 11 in. (280mm) x 3 in. (76mm) x 0.75 in. (19.1mm) (span x depth x thickness) and different fiber volume fractions (ranging from 0% to 1.5%) were prepared. One inch long (25.4mm) brass coated smooth steel fibers with 0.016 in. (0.4mm) diameter were used. Four different series with the same mortar matrix were cast. The mix proportions are listed in Table 2. All the notches were saw-cut and were one inch (25.4mm) deep. These beams were tested after curing for approximately 90 days in an environment with 96% relative humidity and 80°F (26.7°C). All the beams were tested in a servo-controlled closed-loop MTS testing machine. CMOD was used as the feedback signal of the control system. The beams were loaded such that the rate of increase of CMOD was maintained at 2.5×10^{-4} in (6.4×10^{-3}mm) per second. There were 6 beams for each series. A total of 24 beams were tested. At least two beams were loaded cyclically and the rest were loaded monotonically.

DISCUSSION OF TEST RESULTS

The material properties such as K_{Ic}^{s}, $CTOD_c$, α, β, and C of the unreinforced matrix were directly calculated from the experimental results of F0 series and are 775.4 psi $\sqrt{in}$ (0.852 $MNm^{-3/2}$), 0.00025 in. (6.35 x 10^{-3}mm), 7, 1.3, and 1.25 respectively. The Young's modulus for this series was 5.87 x 10^6 psi and was found to be about the same as other series.

To account for distribution of fibers from section to section of the beam, from beam to beam and to include spatial distribution at a given section an effective volume fraction (v_{ef}) rather than global volume fraction (v_f) was used in the theoretical analysis. It was mentioned earlier that for very large CMOD, the matrix contribution can be disregarded, $K_I = 0$, and $P = P_s^f$. For each beam, a value of P_s^f was selected for a very large value of CMOD (see Fig. 1). For this point, since the crack had visibly traversed almost the entire depth of the beam, it was assumed that $\ell_e = .99\ (b - a_0)$. For this ℓ_e, V_{ef} was determined (by iteration process) using Eqs. 3, A9 and A10 (see Fig. A3).

The ranges of effective fiber volume fractions (v_{ef}) are listed in Table 2 in comparison with the actual fiber volume fraction (v_f). It can be seen that v_{ef} ranged about 0.5 v_f to 1.5 v_f which seems reasonable. The experimental results of load-CMOD curves for beams made with different fiber volume fractions (including unreinforced matrix) are plotted in Fig. 6 and compared with the theoretical prediction. The theoetical prediction is judged to be quite satisfactory. Good agreement was also found between the theoretical prediction and experimental results of load-deflection curves (Fig. 7). Fig. 8 shows a plot of the theoretically calculated relative peak load values vs. effective fiber volume fractions. The strength of FRC beams with effective fiber volume fraction of 2.5% is about twice the strength of unreinforced

matrix. The calculated values of energy release rate [G_R ,values at ℓ_e equals 1.8 in, (45.7mm) (a/b = 0.933)] are also plotted in Fig. 8 for different values of v_{ef}. It can be seen that the energy absorption ability for beams with v_{ef} = 2.5% is about 30 times that of unreinforced matrix. In comparison to the improvement of energy absorption, the strength improvement due to addition of fibers is less significant. This was also shown by Shah and Rangan [14].

COMPARISON WITH OTHER EXPERIMENTS

Load-CMOD curves reported by Velazco, et al. [17] were also analyzed. The material properties used to predict the composite behavior were calculated from the reported data and are given in Fig. 9. Experimental results reported by Velazco, et al. [17] are also plotted in Fig. 9. The theoretical predictions are in good agreement with the experimental results for all different effective fiber volume fractions.

CONCLUSIONS

1. A Fracture Model is proposed for fiber reinforced concrete. This model is based on the matrix fracture properties that the crack propagation in the matrix can be described by two parameters: critical stress intensity factor and critical crack tip opening displacement. Because of the nonlinear slow crack growth, two fracture parameters are required. The stress intensity factor is calculated at the tip of the effective crack rather than the initial crack length.

2. Effect of fibers is to reduce the stress intensity factor at the tip of the effective crack and to provide additional energy due to debonding.

These effects can be incorporated in the proposed model if the pull-out load-slip relationship of a single fiber is known.

3. The model predicted load vs. deflection and load vs. crack mouth opening displacement relationship compared favorably with the experiments described here as well as those reported by others.

4. In this investigation only steel fibers and mode I crack propagation are considered.

ACKNOWLEDGMENT

This research investigation was supported by the Air Force Office of Scientific Research under Grant No. AF05R-82-0243 [Lt. Col. Lawrence D. Hokanson, Program Manager].

REFERENCES

1. Ballarini, R., Shah, S. P., and Keer, L. M., "Crack Growth in Cement Based Composites," Engineering Fracture Mechanics, Vol. 20, No. 3, 1984, pp. 433-445.

2. Burakiewicz, A., "Testing of Fiber Bond Strength in Cement Matrix," Proceedings, International Symposium, RILEM-ACI-ASTM, Sheffield, Sept. 1978, pp. 355-365.

3. Bowling, J., and Groves, G. W., "The Propagation of Cracks in Composites Consisting of Ductile Wires in a Brittle Matrix," Journal of Materials Science, Vol. 14, 1979, pp. 443-449.

4. Diamond, S., and Bentur, A., "On the Cracking of Concrete and Fiber-Reinforced Cement," in Application of Fracture Mechanics to Cementitious Composits, ed. by S.P. Shah, to be published by Martinus Nijhoff Publishers, 1985.

5. Foote, R. M. L., Cotterell, B., and Mai, Y. W., "Crack Growth Resistance Curve for a Cement Composite," in Advances in Cement Matrix Composites, Proceedings, Symposium L., Materials Research Society, Annual Meeting, Boston, Massachusetts, Nov. 17-18, 1980, pp. 135-144.

6. Hillerborg, A., "Analysis of Fracture by Means of the Fictitious Crack Model, Particularly for Fiber Reinforced Concrete," International Journal of Cement Composites, Vol. 2, No. 4, Nov. 1980, pp. 177-184.

7. Jenq, Y. S., and Shah, S. P., "Nonlinear Fracture Parameters for Cement Based Composites: Theory and Experiments" in Application of Fracture Mechanics to Cementitious Composites, ed. by S. P. Shah, to be published by Martinus Nijhoff Publishers, 1985.

8. Jenq, Y. S., and Shah, S. P., "A Frcture Toughness Criterion For Concrete," Engineering Fracture Mechanics (to appear).

9. Jenq, Y. S., and Shah, S. P., "A Two Parameter Fracture Model for Concrete," Journal of Engineering Mechanics, ASCE, (MS# 16-2-4.J), April 1985.

10. Johnston, C. D., and Gray, R. J., "Uniaxial Tensile Testing of Steel Fiber Reinforced Cementitious Composites," Proceedings, International Symposium, RILEM-ACI-ASTM, Sheffield, Sept. 1978, pp. 451-462.

11. Lenian, J. C., and Bunsell, A. R., "The Resistance to Crack Growth of Asbestos Cement," Journal of Materials Science, Vol. 14, 1979, pp. 321-332.

12. Naaman, A. E., and Shah, S. P., "Pull-out Mechanism in Steel Fiber Reinforced Concrete," Journal of ASCE-STD, August 1976, pp. 1537-1548.

13. Petersson, P. E., "Fracture Mechanics Calculations and Tests for Fiber-Reinforced Cementitious Materials," in Advances in Cement-Matrix Composites, Proceedings, Symposium L., Materials Research Society, Annual Meeting, Boston, Massachusetts, Nov. 17-18, 1980, pp. 95-106.

14. Shah, S. P. , and Rangan, B. V., "Fiber Reinforced Concrete Properties," ACI Journal, Vol. 62, No. 2, Feb. 1971, pp. 126-135.

15. Stroeven, P., Shah, S. P., deHaan,Y. M., and Bouter, C., "Pull-out Tests of Steel Fibers," Proceedings, International Symposium, RILEM-ACI-ASTM, Sheffield, SEPT. 1978, PP. 345-353.

16. Tada, H., Paris, P.C., and Irwin, G.R., The Stress Analysis of Cracks Handbook, Del Research Corporation, Hellertown, Pennsylvania, 1973.

17. Velazco, G., Visalvanich, K., Shah, S. P., and Naaman, A. E., "Fracture Behavior and Analysis of Fiber Reinforced Concrete Beams," Progress report for National Science Foundation, March 1979.

18. Wecharatana, M., and Shah, S. P., "A Model for Predicting Fracture Resistance of Fiber Reinforced Concrete," Cement and Concrete Research, November 1983, pp. 819-830.

19. Wecharatana, M., and Shah, S. P., "Prediction of Nonlinear Fracture Process Zone in Concrete," Journal of EMD, ASCE,June 1982, pp. 1100-1113.

Appendix

a. LEFM based formulae of 3-PB tests

For the notched beam geometry used in present study [Fig. A1], the $CMOD^e$ can be calculated as follows [9, 16].

$$CMOD^e = \frac{6Ps}{b^2tE'} V_1\left(\frac{a}{b}\right), \quad a = a_o + \ell_e \tag{A1}$$

$$V_1\left(\frac{a}{b}\right) = 0.76 - 2.28A + 3.87A^2 - 2.04A^3 + \frac{0.66}{(1-A)^2}, \quad A = \frac{a}{b}$$

in which $E' = \frac{E}{1-\nu^2}$, E = Young's modulus and ν = Poisson's ratio. The stress intensity factor (K_I) can be expressed as:

$$K_I = \frac{1.5\ Ps}{b^2t} F_1\left(\frac{a}{b}\right) \sqrt{\pi a} \tag{A2}$$

The mathematical expression of crack tip opening displacement (CTOD) can be stated as [9]:

$$CTOD = CMOD^e\left[\left(1 - \frac{a_o}{a}\right)^2 + \left(-1.149\ \frac{a}{b} + 1.081\right)\left(\frac{a_o}{a} - \left(\frac{a_o}{a}\right)^2\right)\right] \tag{A3}$$

The above equations are valid for $\frac{S}{b} = 4$ and gives less than 1% error.

b. Relationship of ℓ_e and K_I at precritical crack growth stage

At precritical crack growth stage the effective crack extension (ℓ_e) and stress intensity factor (K_I) of unreinforced matrix can be empirically related as:

$$\ell_e = \ell_{ec}\left(\frac{K_I}{K_{Ic}^S}\right)^n, \quad 0.5\ K_{Ic}^S < K_I \leq K_{Ic}^S$$

$$\ell_e = 0, \qquad K_I < 0.5\ K_{Ic}^S \tag{A4}$$

where ℓ_{ec} = critical effective crack extension, n = a constant which

depends on the ratio of a_0/b and can be determined by curve fitting the results of P-CMOD curve of unreinforced mortar. It was found that n = 3 for the present study.

c. Relationship between total crack mouth opening displacement (CMOD) and the elastic crack mouth opening displacement ($CMOD^e$)

It was observed from experimental results [8] that the total crack mouth opening displacement (CMOD) and elastic crack mouth opening displacement ($CMOD^e$) can be expressed as:

$$CMOD = CMOD^e \quad , \quad 0.5\ K_{Ic}^S > K_I \tag{A5}$$

$$CMOD = \frac{\alpha}{\alpha-1} CMOD^e, \quad 0.5\ K_{Ic}^S < K_I < K_{Ic}^S \tag{A6}$$

$$CMOD = CMOD^e\left(\frac{\beta}{\beta-1}\right) + CMOD_{max}\left(\frac{\beta-\alpha}{\alpha\beta-\alpha}\right), \quad K_I = K_{Ic}^S \tag{A7}$$

where α and β are material constants and $CMOD_{max}$ is CMOD value at peak load for unreinforced matrix. It should be noted that α is indeed function of K_I and CTOD. For simplicity α is assumed to be constant in present study. Values of α and β are reported in Table 1.

d. Calculation of K_I^f

The stress intensity factor of a crack in an infinite strip of unit thickness subjected to a unit point load (Fig. A2) was used as Green's function to calculate the stress intensity factor due to fiber bridging force (K_I^f) . This K_I^f value can be expressed as [16]:

$$K_I^f = \int_{a_0/a}^{1} 2\sigma(X)F(X,Y)/\sqrt{\pi a}\ aX \tag{A8}$$

where

$$X = \frac{c}{a}$$

$$Y = \frac{a}{b}$$

and

$$F(X,Y) = \frac{3.52(1 - X)}{(1 - Y)^{3/2}} - \frac{4.35 - 5.28X}{(1 - Y)^{1/2}}$$

$$+ \left\{\frac{1.30 - 0.30(X)^{3/2}}{\sqrt{1 - X^2}} + 0.83 - 1.76\ X\right\} \quad \{1 - (1 - X)Y\}$$

$\sigma(X)$ is calculated using the known CMOD value, crack profile and Eq. 3. In the above equation, $\underline{a}$ is given; therefore, X is the only variable. Because of the singularity problem at the integral boundary, the integration was achieved using Gauss-Chebyshev quadrature.

e. Calculation of P_s^f

The value of P_s^f is determined using global equilibrium as illustrated in Fig. A3. The total tension force at the cracked cross-section of the beam is given by:

$$F_T = \int_0^{\ell_e} t\sigma(X)\ dX + \int_{\ell_e}^{\ell_t} t\sigma_c(X)\ dX \qquad (A9)$$

where $\sigma(X)$ is the fiber bridging closing pressure expressed in terms of beam depth, σ_c is the stress in the uncracked portion of the cross-section which is assumed to be linearly related to the beam depth, and ℓ_t locates the neutral axis and can be determined by equating the tensile and the compressive forces on the cross-section. The value of P_s^f is determined from:

$$P_s^f = 4\left[F_T\left(\ell_p + \frac{2}{3}\ (b - \ell_t - a_o)\right)\right] \frac{t}{s} \qquad (A10)$$

where ℓ_p determines the location of the centroid of F_T and can be evaluated from the shape of the closing pressure distribution.

TABLE 1 - RESULTS OF K_{Ic} TEST ON MORTAR*

DIMENSION** S x b x t (in. x in. x in.)	NUMBER Of SPECIMENS	P_{max} (lbs)	K^S_{Ic} ($psi\sqrt{in}$)	$CTOD_c$ ($x10^{-3}$in.)	ℓ_{ec} (in.)	α	β	G^S_{Ic} (lb/in)	G_F (lb/in)	C
2.6 x 9 x 2.375	2	1221	919.5	0.475	0.466	8.5	1.6	0.174	0.36	1.816
24 x 6 x 2.25	2	648	879	0.336	0.274	8.5	1.6	0.146	0.310	1.123
12 x 3 x 1.125	6	217.5	816.3	0.332	0.230	8.5	1.6	0.140	0.296	2.110

* Mix proportion C:S:A:W = 1:2.6:0:0.45

** S = span, b = depth, t = thickness
1 inch = 25 mm, 1000 psi = 6.9 MPa, 1 lb = 0.454 KgW

TABLE 2 - MIX-PROPORTION OF FIBER SERIES

SERIES	CEMENT	SAND* FRACTURE	WATER (V_f)	FIBER VOLUME VOLUME FRACTURE (%)	EFFECTIVE FIBER (%)
F0	1.0	2.0	0.4	0	0
F1	1.0	2.0	0.4	0.5	0.4 ~ 1.1
F2	1.0	2.0	0.4	1.0	0.7 ~ 1.4
F3	1.0	2.0	0.4	1.5	1.4 ~ 2.6

* Maximum aggregate size equals 0.1875 in.
1 in. = 25 mm

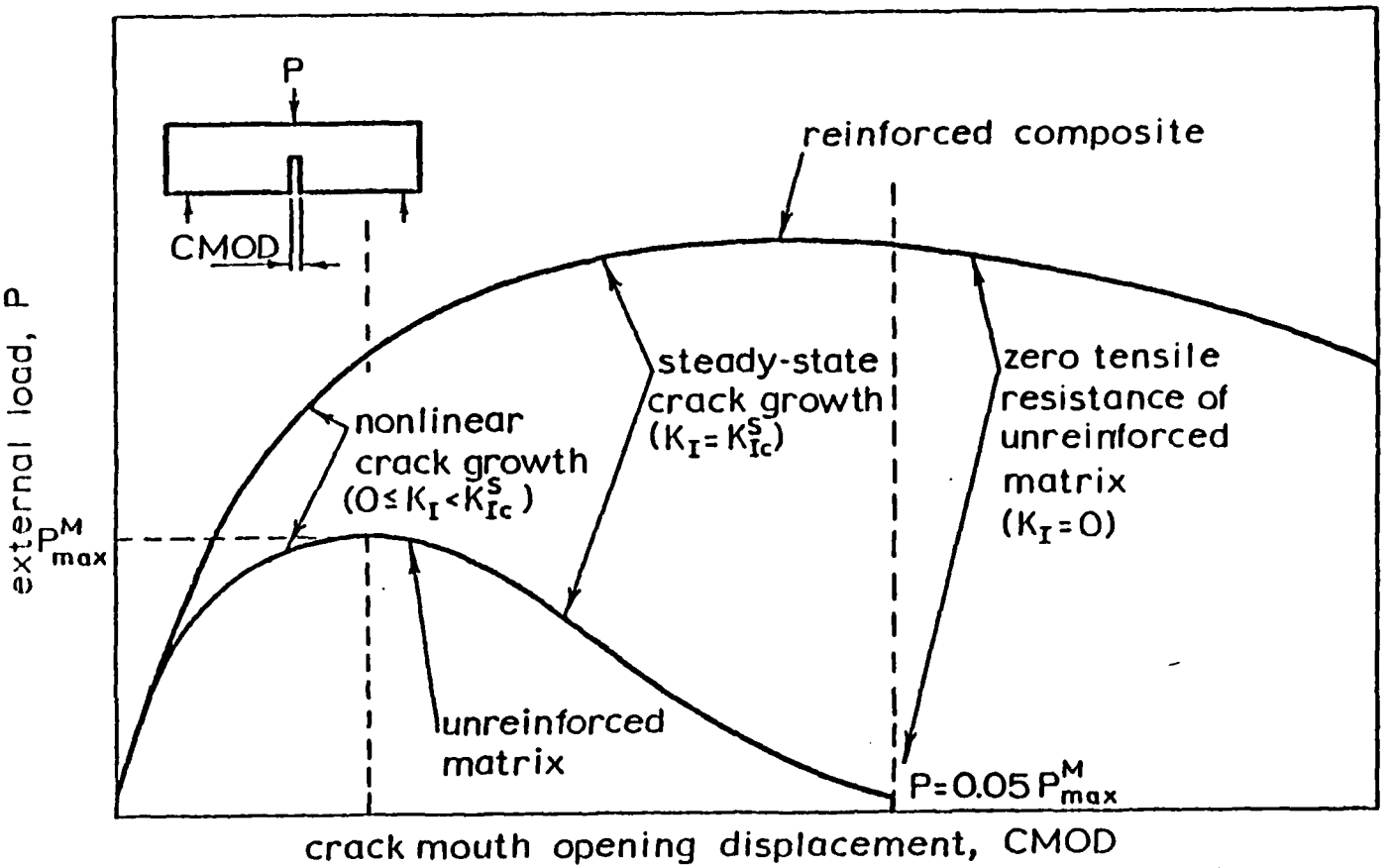

Fig. 1. Fracture Resistance Mechanisms of Fiber Reinforced Concrete

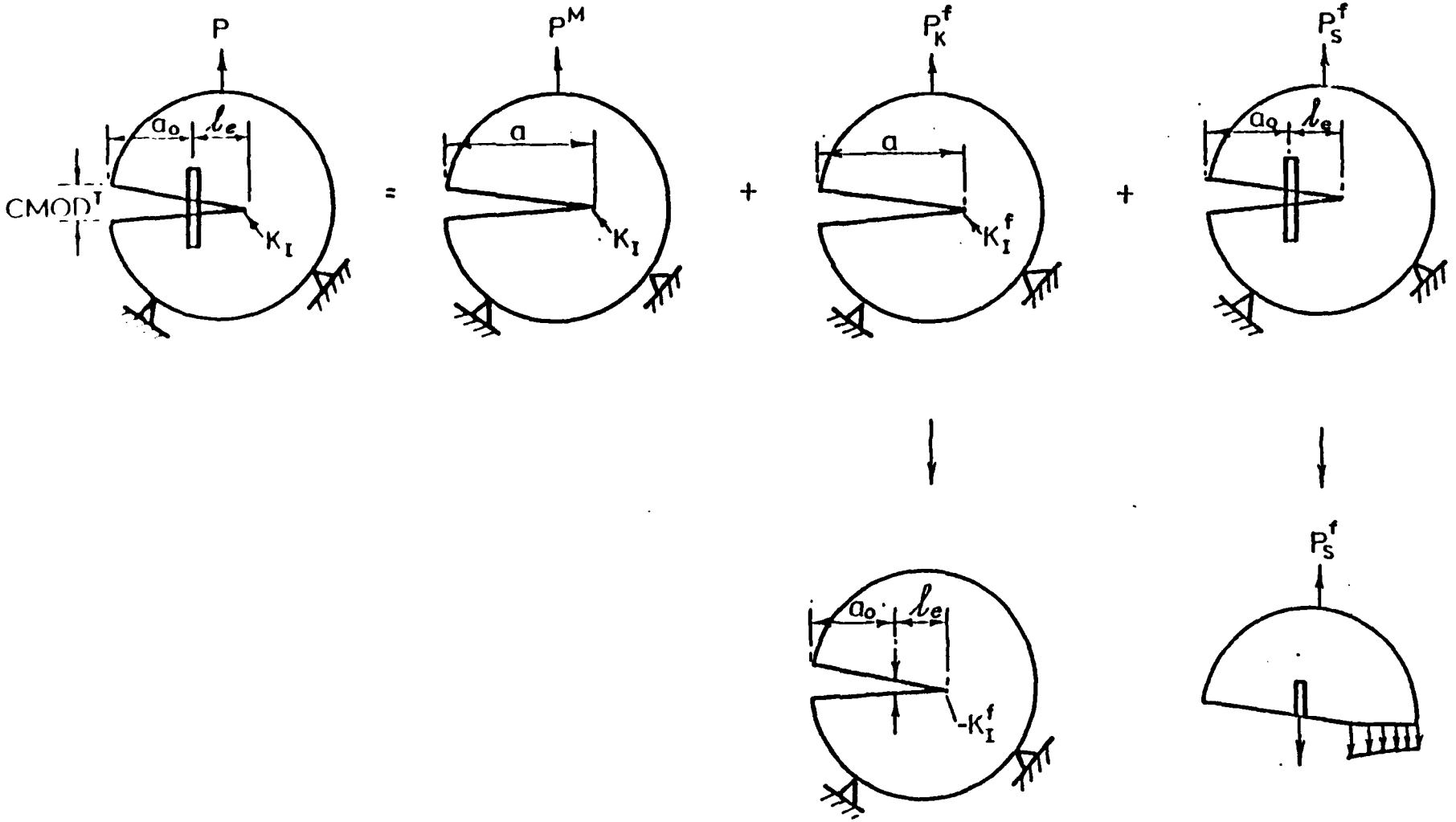

Fig. 2 - Compositions of External Load Applied on a Fiber Reinforced Structure

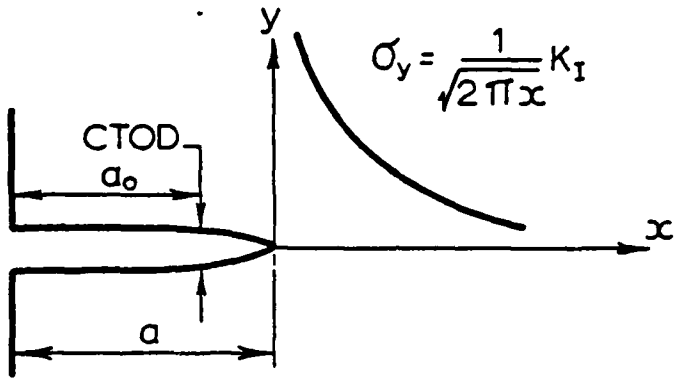

(a) Effective Griffith crack

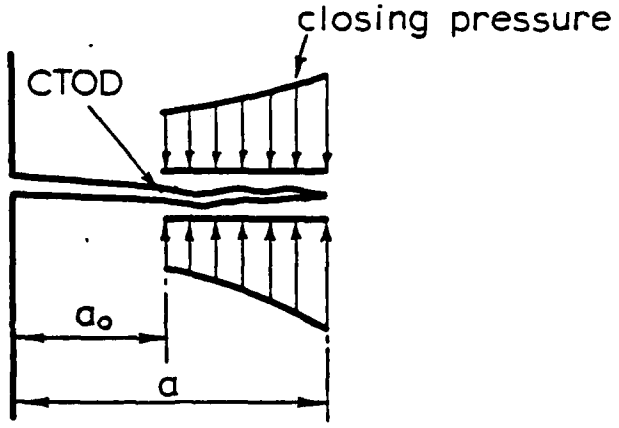

(b) Crack with closing pressure

Fig. 3. Energy Consideration of Stress Singularity and Closing Pressure

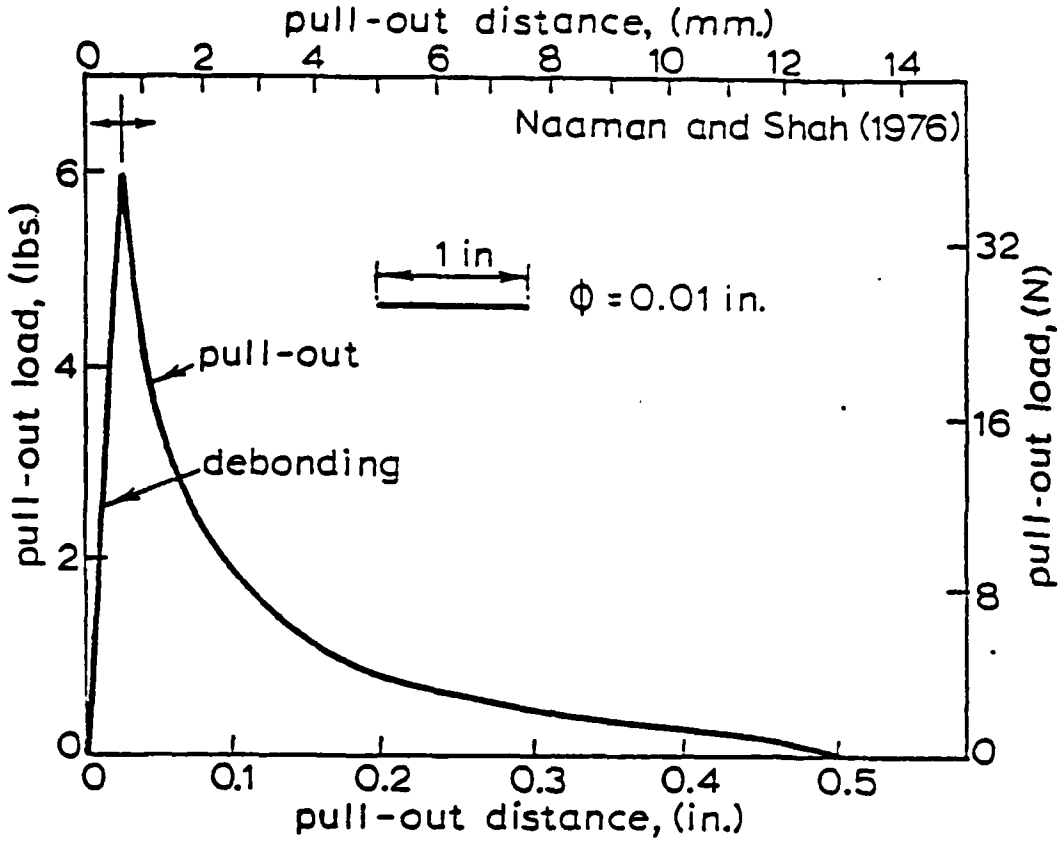

Fig. 4a. Pull-out Load-Slip Relationship of Single Fiber with Hook at the Ends

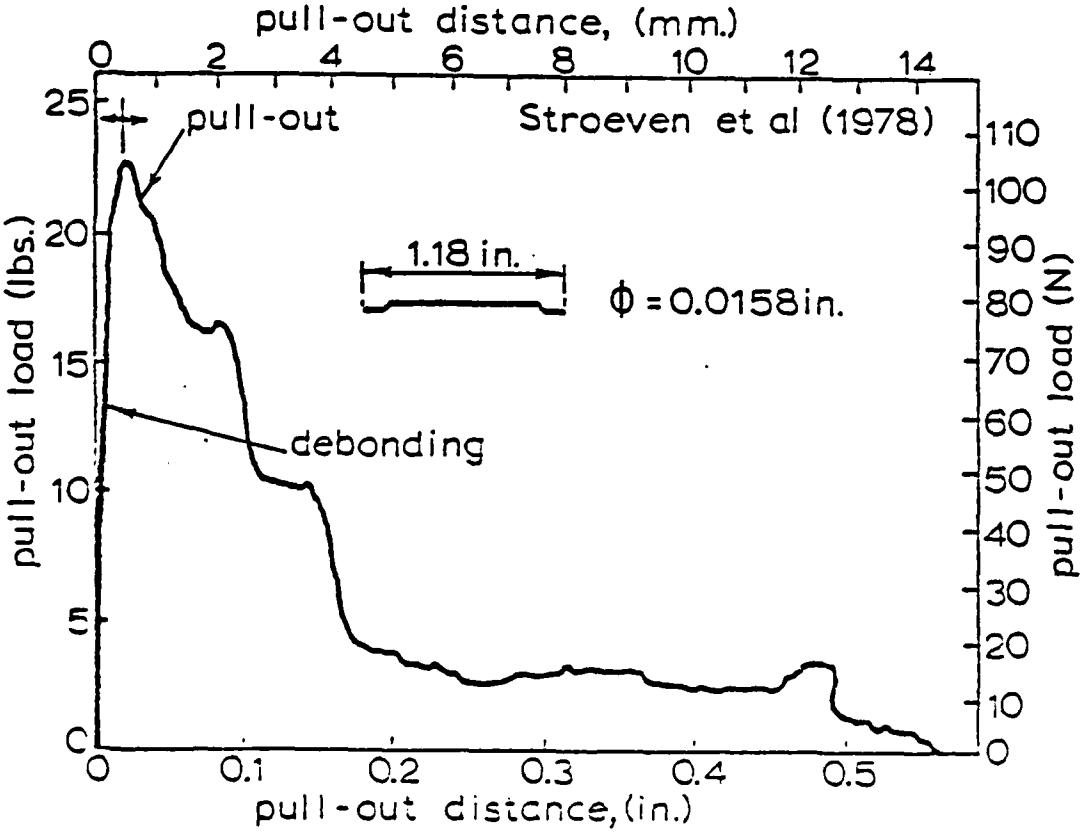

Fig. 4b. Pull-out Load-Slip Relationship of Single Straight Fiber

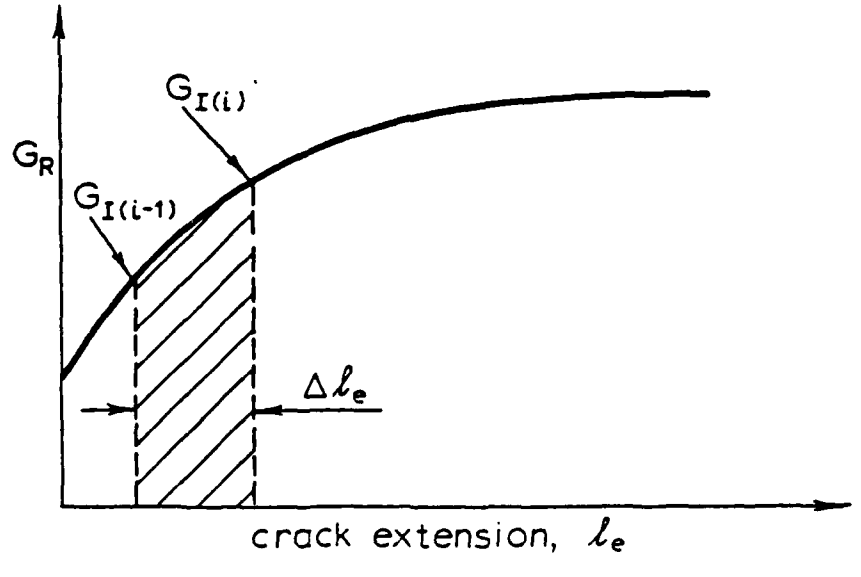

Fig. 5. Consideration of Energy from Load-Deflection and G_R curves

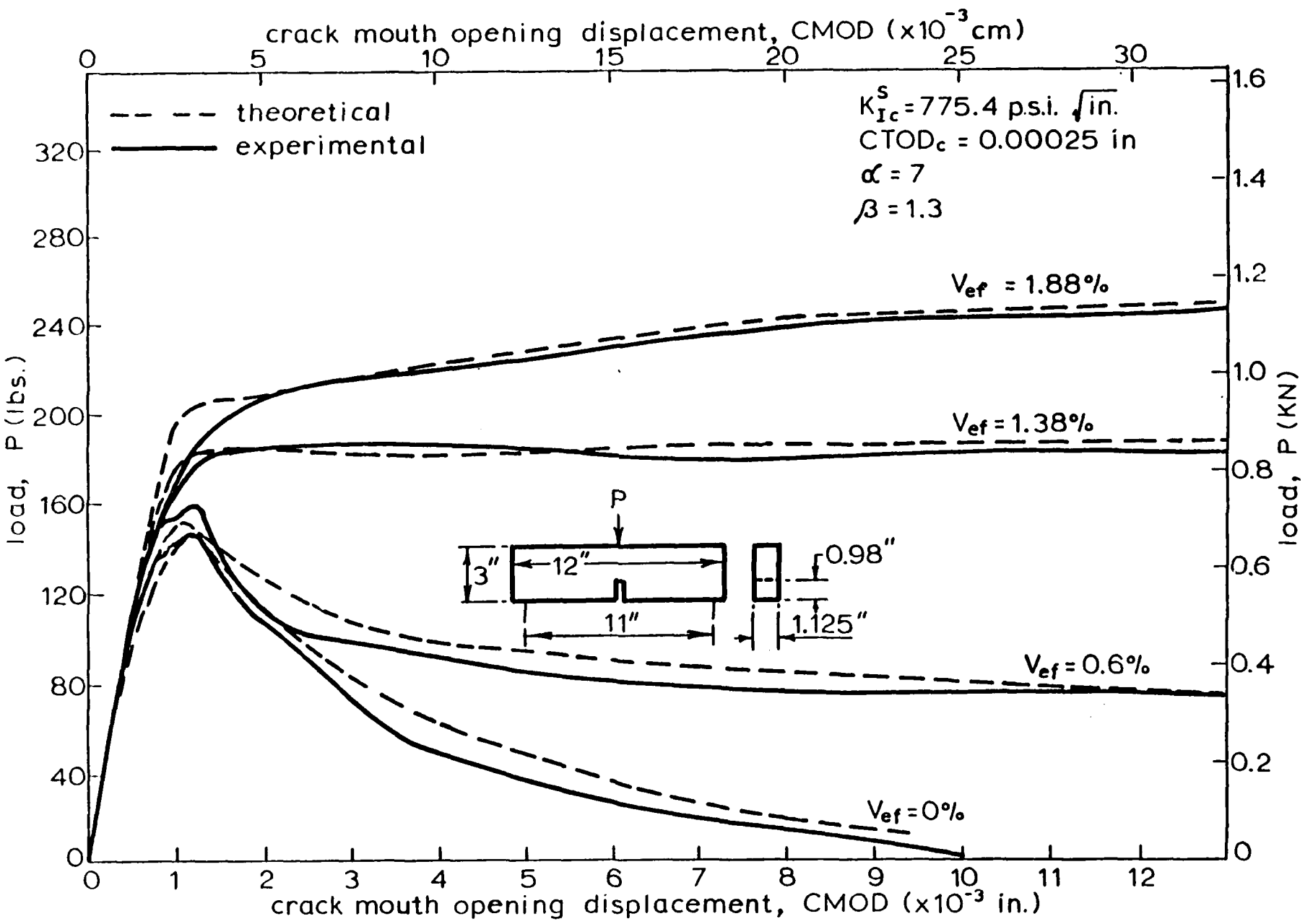

Fig. 6. Comparison of Theoretical Prediction and Experimental Results of Load-CMOD Curve

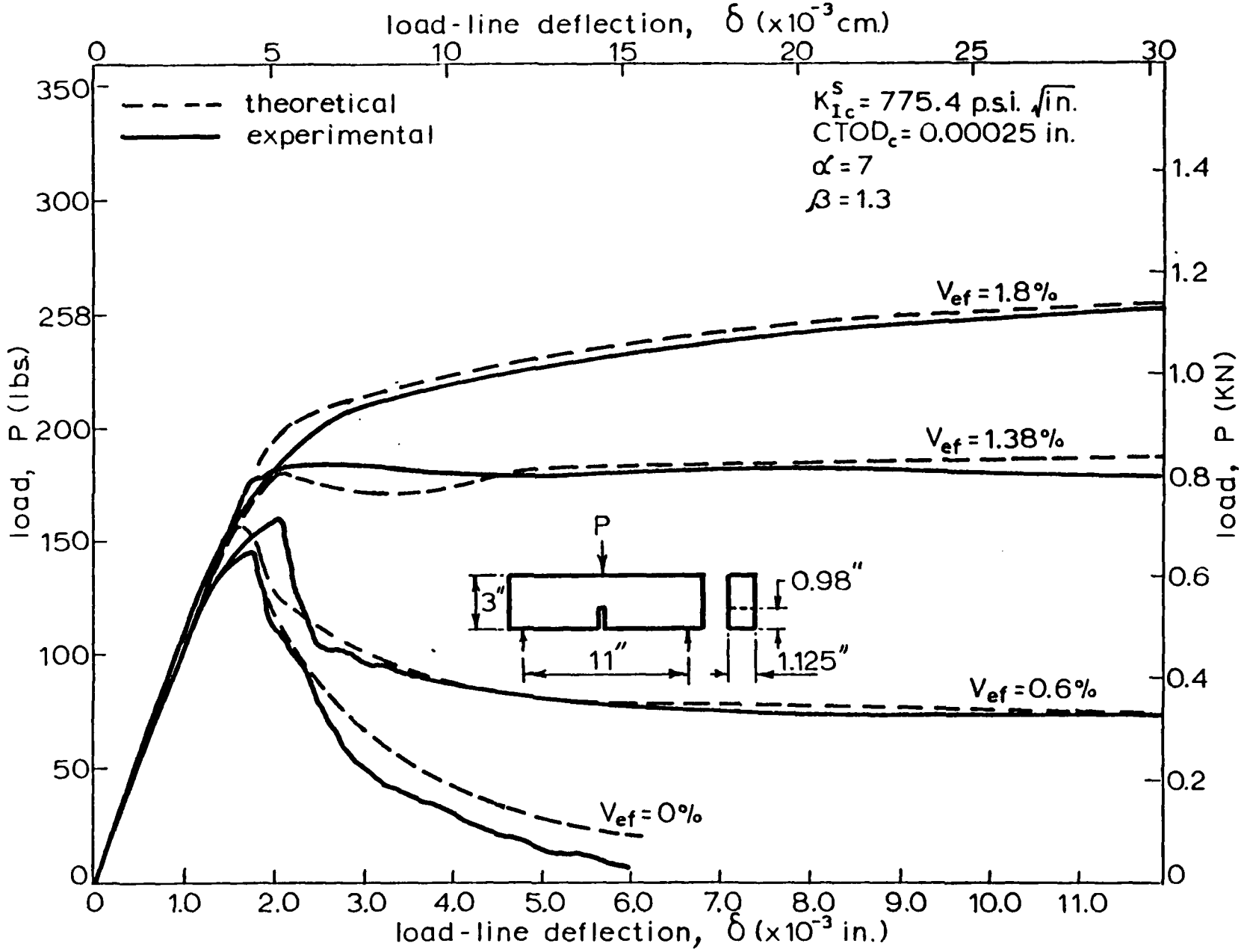

Fig. 7. Comparison of Theoretical Prediction and Experimental Results of Load-Deflection Curve

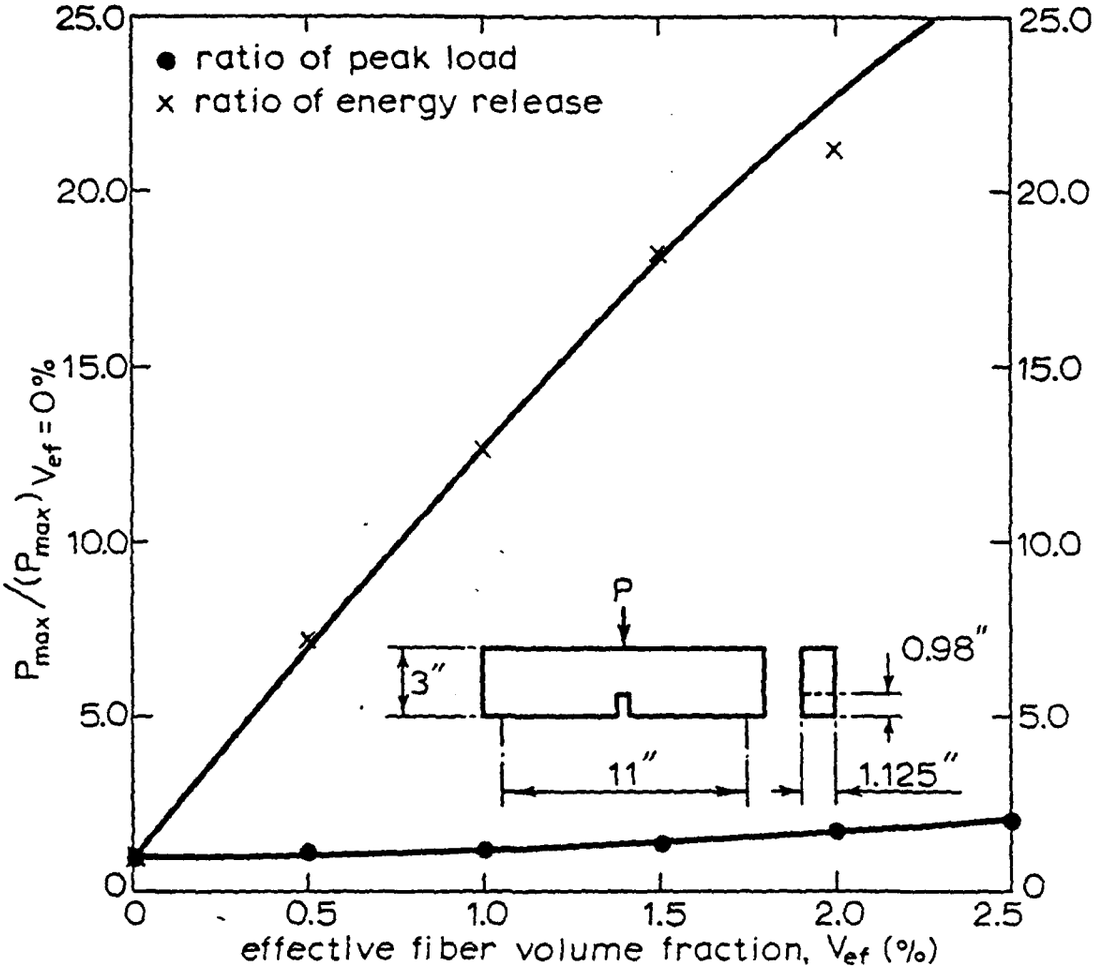

Fig. 8. Theoretical prediction of improvements of energy absorption and strength for different effective fiber volume fractions

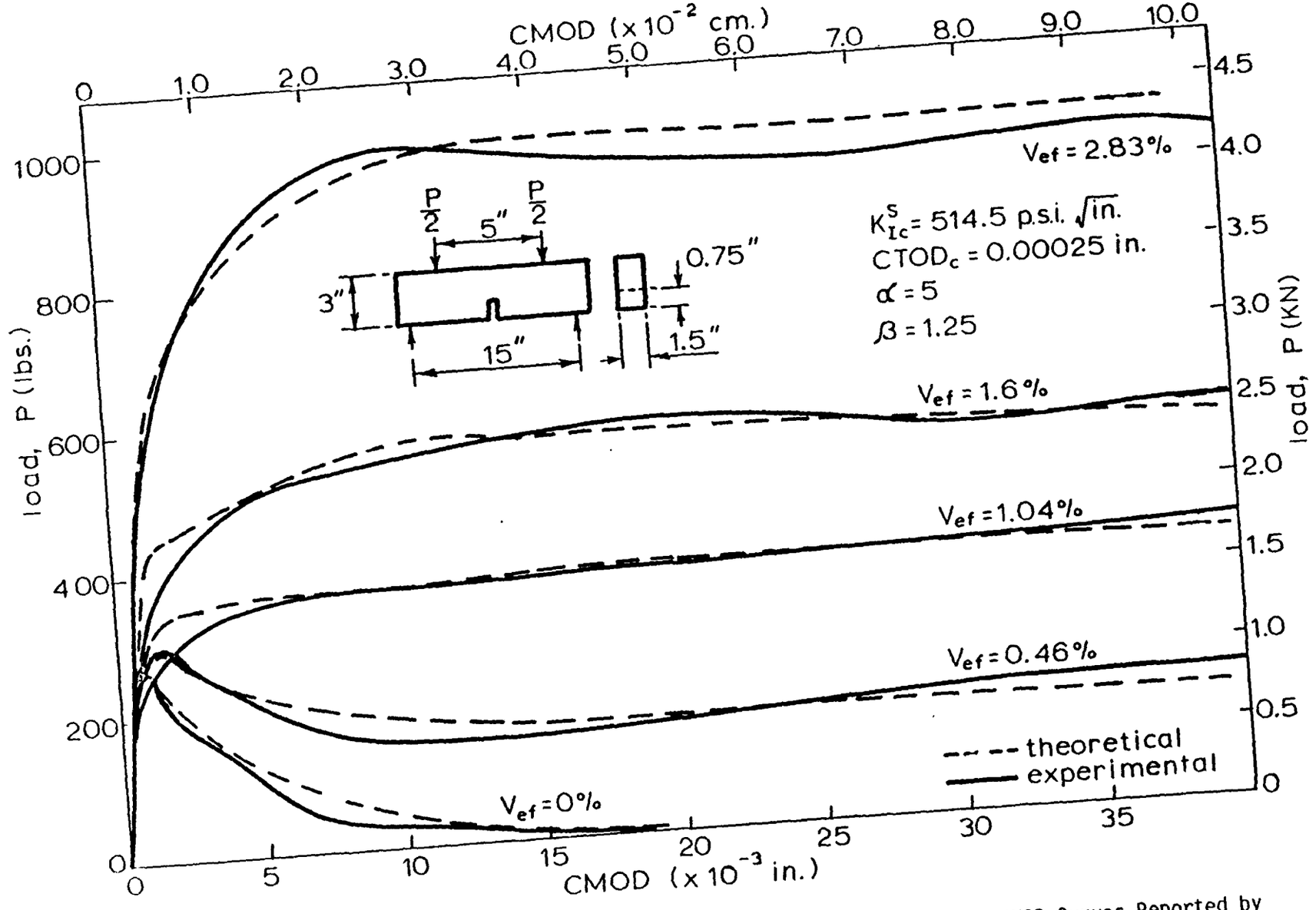

Fig. 9. Comparison of Theoretical Prediction and Experimental Results of Load-CMOD Curves Reported by Valazco et al. [17]

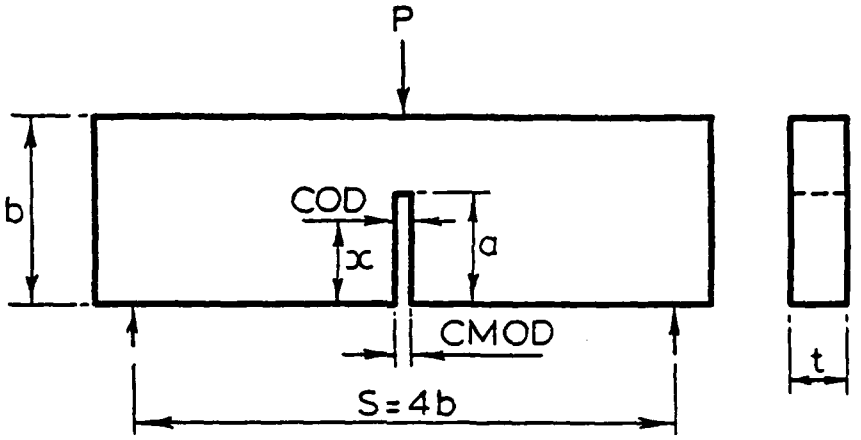

Fig. A1. Dimensions of three-point bend Notched Beam Tests

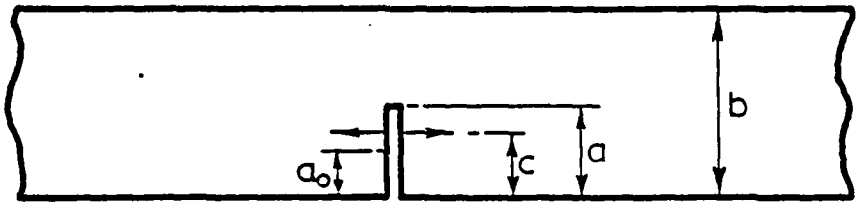

Fig. A2. Stress Intensity Factor of an Infinite Strip Subjected to a Unit Point Load

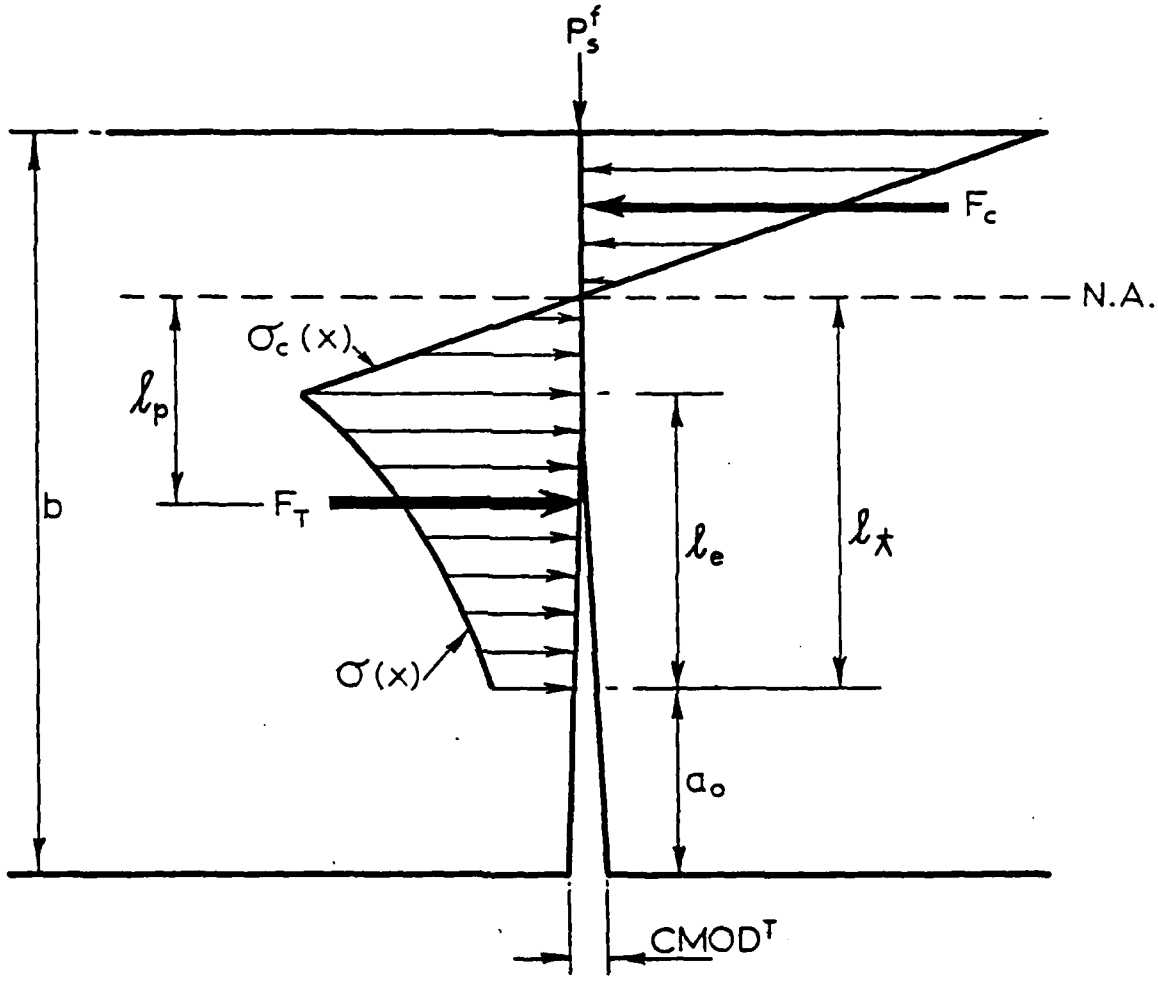

Fig. A3. Global Equilibrium Condtion of 3-PB Notched Beam

END

11-86

DTIC